

USING A RE-ENTRANT MICROWAVE RESONATOR TO MEASURE AND MODEL THE DIELECTRIC BREAKDOWN ELECTRIC FIELD OF GASES

S. K. Remillard and A. Hardaway

Department of Physics
Hope College
27 Graves Place, Holland, MI 49423, USA

B. Mork, J. Gilliland, and J. Gibbs

Department of Chemistry
Hope College
35 East 12th Street, Holland, MI 49423, USA

Abstract—A gas will breakdown in a high electric field and the mechanisms of this breakdown at DC and high frequency fields have been an object of study for the past century. This paper describes a method to induce breakdown in a uniform microwave field using a re-entrant sub-quarter wave resonator. Slater's theorem is used to determine the magnitude of the threshold electric field at which breakdown occurs. The breakdown threshold is modeled using the effective electric field concept, showing that breakdown varies with pressure as $E_{bd} = CP^m \left(1 + (\omega/B \cdot P)^2\right)^{1/2}$ where P is the pressure, B and C are fit parameters, and m was found experimentally to equal $1/2$. This function exhibits a minimum at $P_{\min} = \omega/B$. Breakdown data from the literature for nitrogen at various microwave frequencies were found to exhibit breakdown minima at the pressure predicted by our own determination of B , further validating the model.

1. INTRODUCTION

Operation of air-filled radio frequency (RF) and microwave devices in a reduced pressure environment enhances the hazard of dielectric breakdown in a gaseous medium [1]. The microwave breakdown

Corresponding author: S. K. Remillard (Remillard@hope.edu).

strength of the gas is useful information for high power filter and antenna engineering [2], and is also rich in scientific merit. Porteanu, et al. [3] are currently using microwave induced plasmas to build models of the conductivity and dielectric constant of a plasma. Kuo's [4] work explores harnessing the nonlinearity of the plasma in the ionosphere to couple different branches of the plasma dispersion curve, part of a broader effort to use high power microwaves to modify the ionosphere for long range radio propagation. Similarly, an intriguing series of applications certainly arises from Gurevich's studies of stratospheric air breakdown and the resulting ozone generation [5].

This work examines microwave induced dielectric breakdown of gases in a uniform electric field. Cavity resonators have often been used [2,6], but field distributions are inhomogeneous, resulting in a spatially dependent ionization rate and breakdown which is strongly influenced by the diffusion of charged particles out of the high electric field region. On the other hand, a resonant structure is beneficial because of the high electric field that is achieved with modest input power.

We begin with a description of the physical mechanism involved in the microwave induced breakdown of a gas. The breakdown condition is a function of gas pressure, gas composition, microwave frequency, as well as the dimension of the space in which the microwave electric field is particularly large. Next we describe a re-entrant resonator which supports a uniform, high electric field where microwave gas breakdown can be carefully examined under continuous wave conditions. Finally, we present microwave breakdown measurements inside this gap and compare it to measurements made in a TM_{010} parallel plate resonator.

2. BREAKDOWN PHYSICS

2.1. Processes during Microwave Breakdown

When exposed to a sufficiently strong electric field, a gas can become conducting. The onset of high conductivity in a gas occurs suddenly during an electron avalanche process referred to as *breakdown*. A real gas is composed not only of the expected constituent atoms or molecules, but also of a small number of ionized atoms or molecules and free electrons. Both gases and plasmas are electrically neutral, containing free electrons and ions in equal numbers. In the case of a gas, the existing charges are referred to as the *background ionization*. In the presence of an electric field, free electrons accelerate and collide with neutral molecules, sometimes producing an ionization. Because ionization produces more free electrons, the populations of electrons and ions can grow exponentially with time, a process referred to

as dielectric breakdown. This sub-section presents some important aspects of the accepted phenomenology for the breakdown of a gas under a high frequency field.

Due to the small mass of electrons, compared to ions, it is the electrons that accelerate in the electric field and collide with the neutral atoms. At low energies, elastic collisions occur only exchanging kinetic energy, but not converting kinetic energy. At higher energies, the collisions are inelastic. In an inelastic electron-atom collision, some of the electron's kinetic energy is converted into internal energy of the atom by exciting one of the atom's electrons into a higher energy state. The excited states of gas molecules can be electronic excitation (infrared through ultraviolet emission), vibrational excitation (infrared emission) and rotational excitation (microwave emission) [7]. The visible glow of a plasma is due to excited atomic electrons returning to lower energy states and emitting a photon. If the free electron's kinetic energy exceeds the ionization energy of the atom, then an inelastic collision can also remove an electron from the atom, creating another free electron. As ionizations continue, the density of free electrons grows, finally leading to the electron avalanche known as breakdown.

The electric field which induces breakdown is referred to as the *dielectric strength* in the context of DC or low frequency fields, and often as the *threshold field* in the context of microwave frequencies. The threshold field depends on the gas pressure, and in a confined space, dielectric breakdown is divided into two pressure regimes. The breakdown processes are distinctly different depending on the pressure range. At low pressure, charged particles are unlikely to collide with atoms or molecules. At high pressure the collisions are too frequent for the charged particles to accelerate to sufficient kinetic energy for ionization to occur.

Breakdown at microwave frequencies occurs under the influence of different mechanisms than breakdown at DC. For example, at DC and low frequencies secondary electrons emitted from the electrode material are crucial sources of free charge leading to the avalanche current. Secondary electrons are ineffective at microwave frequencies because the free electrons diffuse to the metal surface at the same rate that they leave the metal surface. Sato [8] was nevertheless able to show that the first Townsend ionization coefficient obtained from DC Paschen curves predicts the pressure at which microwave breakdown is a minimum.

While exposed to a low frequency electric field, the electrons readily accelerate under the influence of the conservative electric field. At microwave frequencies the electrons gain kinetic energy with poor efficiency. The oscillatory movement of the electrons is out of phase

with the high frequency field, reducing the work done by the microwave electric field on the electrons. In simple terms, the electrons cannot keep up with the oscillating field. Imagine pushing a child on a swing. If the push is not delivered at the high point of the oscillation, the amplitude of the oscillation does not grow as readily. It is this inefficient transfer of energy to free electrons in the gas that causes microwave breakdown to occur only at very high fields when the gas pressure is very low.

This inefficiency is relieved at high gas pressure. The larger number, N_a , of neutral atoms per unit volume, and hence the shorter mean free path between collisions, ℓ , results in a higher collision frequency, ν_c , between electrons and neutral atoms. Following an elastic collision, the electron begins to accelerate with the electric field, allowing it to efficiently gain kinetic energy from the microwave field. So at high pressure, the electrons gain kinetic energy from a microwave electric field with equal efficiency as with a DC field. However, the short mean free path reduces the mean kinetic energy of the collisions, thus reducing the probability of ionization. For this reason, when gas pressure is high, microwave breakdown occurs only under very high fields.

The inefficient energy transfer resulting from out-of-phase oscillation of the electron in the microwave field is accounted for by an effective electric field [9],

$$E_{eff}^2 = E^2 \frac{\nu_c^2}{\nu_c^2 + \omega^2} \quad (1)$$

which depends on collision frequency, ν_c . E is the applied electric field. E_{eff} is the low frequency electric field that would produce the same kinetic energy that the electron actually gains from the high frequency electric field.

The collision rate increases linearly with the atomic number density of neutral atoms, measured in atoms/m³, or $\nu_c \propto N_a$. Per the ideal gas law, at constant temperature N_a is proportional to pressure, P , so $\nu_c \propto P$. On inspection of Equation (1), E_{eff} clearly approaches the applied electric field at high pressure, or at low angular frequency, ω . At low pressure, and hence low ν_c , the effective electric field is attenuated by the ratio of collision frequency to microwave frequency as $E_{eff} = E \cdot (\nu_c/\omega)$. So, at low pressure, the absence of neutral atoms available for collision with electrons results in a very small value of ν_c and causes the electrons to accelerate as if they are in a much smaller electric field.

The threshold electric field also depends on whether or not free electrons remain in the high electric field region. If the region is small,

then electrons will tend to exit the high electric field by diffusion, causing the threshold electric field to increase due to the reduction in free electron concentration. The free electrons can diffuse into a low electric field region, or they can diffuse to the conducting surfaces and be absorbed. For these reasons, it is more difficult to achieve DC breakdown with either very large or very small electrode spacing.

An important gas dimension is derived from the diffusion process of the electrons. The number density, or rather concentration, of electrons, n_e , at a point in space will be subject to change with time if the concentration is not uniform. Consider a cloud of electrons. If at time, $t = 0$, there is a concentration, n_o , of electrons in the cloud, over time electrons will diffuse out of the cloud and the concentration will fall as [10]

$$n_e(t) = n_o e^{-Dt/\Lambda^2} \quad (2)$$

where D is the diffusion coefficient (SI units m^2/s) and Λ is called the *characteristic diffusion length*. Forcing the number density to be zero at the edge of the electron cloud helps to correlate Λ with the physical extent of the electron cloud. For a cloud of electrons (or a plasma) confined in a gap between two circular plates of radius, R , and separation, d , the characteristic diffusion length was shown by MacDonald [10] to be

$$\Lambda = \left[\left(\frac{2.405}{R} \right)^2 + \left(\frac{\pi}{d} \right)^2 \right]^{-1/2}. \quad (3)$$

This expression is imprecise when the gap becomes as large as the plate diameter because its derivation assumes a cylindrical wall boundary, which is absent for a gap. The threshold electric field, E_{bd} , increases with Λ for small values of Λ below about 1 cm [10]. For longer values of Λ , the breakdown field strength does not depend strongly on Λ . This Λ dependence is a matter of importance in the study of microgap discharges in MEMS devices [11].

As the microwave electric field in a gas increases, eventually a condition is reached where breakdown is favorable. When the creation of free electrons outpaces the loss of free electrons, a runaway build-up occurs. The rate of change of electron density must be positive, and is

$$\frac{dn}{dt} = \gamma n \quad (4)$$

where γ is the electron growth constant. The solution to Equation (4) is clearly exponential, $n = n_o e^{\gamma t}$, where a positive γ corresponds to runaway growth of n . The breakdown condition is defined by $\gamma = 0$.

The growth constant is the sum of several rates: the rate of creation of electrons (ionization), and the rate of electron loss through various mechanisms (diffusion, attachment, and recombination) [10]. In a small plasma, as reported here, diffusion is likely to dominate, at least at low pressure. However, in electronegative gases such as O_2 and SF_6 , attachment will play a significant role. Combining all of the rates [10],

$$\gamma = \nu_i - \nu_a - \frac{D}{\Lambda^2} \quad (5)$$

where $\nu_i = h_i \nu_c$ is the ionization rate, with h_i being the ionization efficiency. The ionization efficiency is the probability that a collision will result in ionization. ν_a is the attachment rate, which is the rate that free electrons attach to neutral atoms to form negative ions. Another electron loss mechanism is recombination, which is the capture of free electrons by positive ions. Recombination affects the energetics of maintaining a plasma, but is insignificant below E_{bd} , so it does not influence the breakdown condition [10].

The combination of the physical processes which contribute in different strengths in different pressure regimes produces a function with a minimum for E_{bd} versus pressure. Breakdown is achieved with a lowest value of E_{bd} right around 1 torr of gas pressure, as shown in Figure 1. At DC the curve follows the law published by F. Paschen [12] in 1889, which describes a universal rule for the breakdown of gases in an electrode gap, d in meters, at pressure, P in

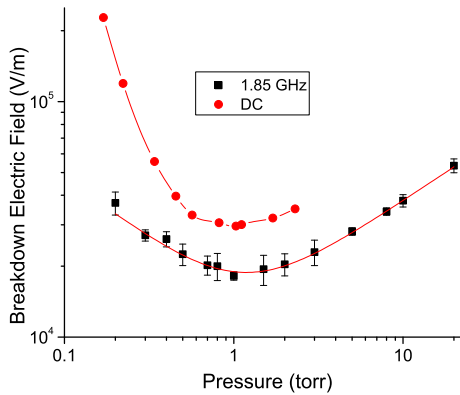


Figure 1. The breakdown electric field of nitrogen has a minimum in pressure dependence at around 1 torr for both DC and 1.85 GHz. The 1.85 GHz data was measured at about 260 K and includes the model fit discussed in this paper.

torr, as $E_{bd} = Pa/(b + \ln(Pd))$, where a and b are free fit parameters. This is an empirical description of DC breakdown, and does not fit breakdown at microwave frequencies, even though Paschen's law also produces a breakdown minimum at a pressure of about 1 torr. The minimum, referred to as the Paschen minimum at DC, is frequency dependent in the microwave range. A breakdown curve, which shows E_{bd} versus pressure, at 1.85 GHz exhibits a slightly different minimum, and a different level of E_{bd} than it does at DC, as seen in Figure 1, owing to the different processes dominating at low and at high frequencies. The DC data in this Figure 1 was adapted from Figure 1 in Miller [13] using the same 8.8 mm gap as the microwave data in Figure 1 of this paper. Coincidentally, breakdown at 1.85 GHz has a minimum at almost the same pressure as Paschen's law. This pressure at the breakdown minimum will be shown later to depend on frequency in the microwave range.

2.2. Model of the Microwave Breakdown Condition

The condition for breakdown is stated exactly as $\gamma > 0$. However, for the experimentalist, breakdown is seen to occur when the microwave electric field exceeds a threshold level, E_{bd} . We model the breakdown condition in terms of the microwave field by postulating that the effective electric field of Equation (1), becomes smaller at lower pressures. Recall that there is an effective electric field because without collisions the free electrons are stuck moving out of phase with the electric field, unable to gain kinetic energy. Only through electron-atom collisions are the electrons able to respond to the electric field. So we begin the model with the simple postulate that the effective electric field at breakdown depends in some way on the number density as

$$E_{eff,bd} \propto N^m \quad (6)$$

where N is the number of neutral atoms or molecules per unit volume. The exponent m remains to be determined. At the low pressures where we will work, the ideal gas law prevails, and $N = P/(k_B T)$, where P is pressure, T is temperature (in Kelvin) and k_B is Boltzmann's constant, so $E_{eff,bd} \propto P^m$. This postulate is combined with Equation (1) to give

$$E_{bd} = CP^m \sqrt{1 + \frac{\omega^2}{\nu_c^2}}. \quad (7)$$

The coefficient, C , has been found in data published for open air breakdown [14] to depend very weakly on the frequency when the frequency exceeds the collision frequency, which becomes the case at

pressures above a couple of torr [15]. Gurevich [14] uses a variation of this model for breakdown in open air specifically with $m = 1$ and also reports that the coefficient varies with gas pressure.

The collision frequency depends on N as $\nu_c \propto N$, and also therefore as $\nu_c \propto P$. But it also depends on the electron energy when the electron energy is high. At fields below E_{bd} , and at pressures below about 100 torr, we will take the collision frequency to depend solely on number density, e.g., we will assume the electron energy distribution is Maxwellian [16]. Including this dependence in Equation (7) gives

$$E_{bd} = CP^m \sqrt{1 + \frac{\omega^2}{(B \cdot P)^2}} \quad (8)$$

which by no accident resembles a similar model used by Gurevich [14] for microwave breakdown in free space, to which this model offers a generalization through the exponent, m , to account for breakdown in confined spaces. This is the working equation with which the pressure dependence of E_{bd} is modeled. It was constructed above from the effective electric field concept of Equation (1), where the pressure dependence of the effective electric field was given a general power law dependence, $E_{eff,bd} \propto P^m$. Equation (8) is graphed qualitatively in Figure 2. The two curves depict the function for the cases that $m = 1$ (suitable for Gurevich's model for free space breakdown), and $m = 1/2$. In the case that $m = 1/2$, the minimum observed in Figure 1 is reproduced, whereas when $m = 1$ E_{bd} levels off at low pressure and exhibits no minimum.

The pressure where a minimum occurs is found by setting the derivative, dE_{bd}/dP , equal to zero, resulting in the very simple prediction of linear frequency dependence of P_{min} , the pressure where E_{bd} has its minimum

$$P_{min} = \sqrt{\frac{1-m}{m}} \frac{\omega}{B}. \quad (9)$$

If $m = 1$, then $P_{min} = 0$ as reported by Gurevich. If $m = 1/2$, then $P_{min} = \omega/B$. Regardless of the value of m , the pressure where the minimum occurs should be proportional to frequency, a point that appears to have been previously made by Raizer [17], although in that treatment, frequency was being swept at constant pressure. Microwave breakdown data such as that shown in Figure 1 can be fit to Equation (8) and the fit values of m and B can be used with Equation (9) to predict P_{min} at other frequencies.

The model of Equation (8) should be considered valid only over small pressure ranges where data are used to fit the model. For

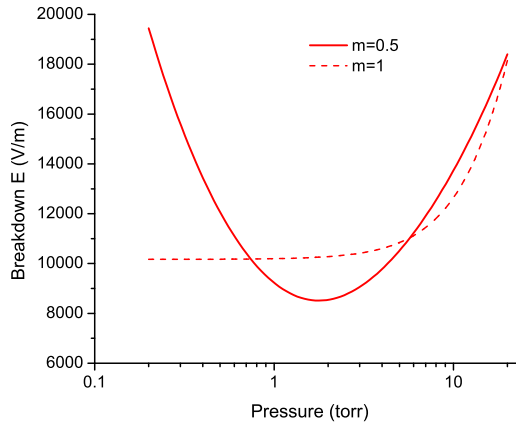


Figure 2. Qualitative graph of the model Equation (8). Parameters were selected to produce breakdown curves which resemble experiment. Most notable is the absence of a minimum when $m = 1$, which corresponds to an open air discharge.

example, there is no physical basis to expect a general power law, $E_{bd} \propto P^{0.5}$ for the case that $m = 1/2$, which Equation (8) yields at pressures which are very high, and beyond the scope of our data. The key applications of Equation (8) will be to model the threshold electric field in the region of the minimum, to predict the pressure at which the minimum occurs, and to provide an electrodynamic description of the transition from a collisionless (less than about 1 torr) to a collisional (greater than about 1 torr) microwave breakdown.

3. MICROWAVE RESONATOR MEASUREMENTS

3.1. Overview of the Re-entrant Quarter Wave Resonator

A foreshortened, sub-quarter-wave quasi-TEM mode cavity is used to set up resonance with a uniform high electric field region. This re-entrant cavity, described electromagnetically using finite element analysis in Reference [18], is illustrated in Figure 4, which will be discussed in Section 3.3. A square cavity, $5\text{ cm} \times 5\text{ cm} \times 5\text{ cm}$ is formed by OFHC copper walls. A solid OFHC copper rod 1 cm in diameter is attached in the center of one of the walls and supports a quasi-transverse electromagnetic (quasi-TEM) resonance. Most data were taken with a rod length of 3.4 cm, which resonates in the fundamental at 1.85 GHz. In a TEM mode, the magnetic and electric fields are both in a plane perpendicular to the rod. Deviation from ideal transversality

occurs due to the finite gap which exists between the end of the rod and the far housing wall. The electric field in this gap is perpendicular to the flat cylindrical end of the rod, which forms a parallel plate capacitor with the housing wall. The capacitance of the gap loads the resonant circuit, reducing the resonant frequency. Adjustability of the gap size, d , is typically used to tune a re-entrant resonator. A conducting disk tuner fixed onto a brass screw is used to adjust the gap size. With an infinite gap size, the rod length would be $d = \lambda/4$, or one quarter of a wavelength long. In our measurements with a 34 mm long rod, the gap was varied from 3 mm to 9 mm, producing a frequency tuning range of 1.5 GHz to 1.85 GHz. Due to the capacitive loading, the rod length is shorter than $d = \lambda/4$, where λ is the free space wavelength. The electric field is much stronger inside the gap than anywhere else in the resonator, and it is quite uniform with electric field lines crossing between the end of the rod and the tuning disk, alternating in direction at the microwave frequency. It is in this capacitive gap that the microwave breakdown occurs. A method is then needed to determine the electric field strength in the gap.

3.2. Using Slater's Theorem to Compute the Electric Field in the Gap

The electric field inside a microwave resonator can be determined analytically, provided there is an analytic solution to Maxwell's equations. All microwave breakdown data known to the authors were acquired in systems with analytic field solutions. However, while researching this writing, a paper was found by Rose and Brown [19] from 1952 suggesting the use of perturbation theory to measure the fields at microwave breakdown. Subsequent result published by Rose and Brown however, used a TM_{010} parallel plate resonator, with analytic electric field calculations.

The electric and magnetic fields inside a resonator have a complicated spatial variation, which nevertheless satisfies the Helmholtz wave equation under the constraints of the conductive boundary conditions. Analytic solutions of the electric and the magnetic fields exist only for a few simple cavity geometries. It is not usually possible to analytically find the magnitude of the fields inside most resonators, let alone their geometric distribution. The field strength can be determined numerically using full-wave electromagnetic field simulation, as was done for example in Reference [20], or experimentally using a network analyzer, as is describe here.

The perturbation theory of Slater is used here to measure the local electric field. A small piece of known dielectric material is placed inside

the gap of an empty re-entrant resonant cavity. The small dielectric slightly disturbs, or rather perturbs, the local electric and magnetic fields concentrating the electromagnetic field energy in the dielectric and causing an apparent shift in the resonator volume.

Only a small fraction of the empty space inside an electromagnetic resonator is filled with the dielectric material with relative permittivity, ε_r , and relative permeability, μ_r . The interaction between the magnetic permeability of the material and the magnetic field of the resonator will cause the reactance to increase and thus raise the resonant frequency by the inductive loading. Likewise, the interaction between the electric permittivity of the material and the electric field of the resonator will cause the reactance to decrease and thus lower the resonant frequency by the capacitive loading. This frequency shift, $f_o - f$, was first described by Maier and Slater [21], and has come to be known as Slater's theorem

$$\omega^2 = (2\pi f)^2 = \omega_o^2 \left[1 + \frac{\int_{\text{dielectric}} (\mu_o \mu_r H^2 - \varepsilon_o \varepsilon_r E^2) dV}{\int_{\text{cavity}} (\frac{1}{2} \mu_o H^2 + \frac{1}{2} \varepsilon_o E^2) dV} \right] \quad (10)$$

where H and E are the magnetic and electric fields, which are position dependent. $\omega_o = 2\pi f_o$ is the original, unperturbed angular frequency. The top integral is evaluated over the dielectric perturbation, and gives the energy stored in the perturbation. The bottom integral is evaluated over the entire empty cavity and is equal to the peak energy stored per cycle in the resonator, or U_o .

When evaluating the top integral, it is often possible to neglect the integral over the magnetic fields. For the purpose of measuring the microwave threshold field of the gas that fills the resonator volume, we are concerned with the electric field in the gap, which is a region of very low magnetic field. Neglecting the magnetic field integral in the numerator of Equation (1) is justifiable only if H is negligible inside the dielectric perturbation. The magnetic field in the gap of a re-entrant resonator is due to the displacement current. A 3 mm PTFE Teflon cylinder ($\varepsilon_r \approx 2.1$, $\mu_r = 1.0$) was placed in the center of the 10 mm diameter electric field region and used as the perturbation. Evaluation of the Maxwell-Ampere law in the gap at 1.8 GHz reveals that $\int \mu_o \mu_r H^2 dV \approx (2 \times 10^{-4}) \cdot \int \varepsilon_o \varepsilon_r E^2 dV$. From this we find that, ignoring the magnetic perturbation in these measurements, there is a systematic error in the electric field of about 0.01%.

In a small electric-field-only perturbation in the gap, the electric field can be treated as uniform over the volume of the dielectric.

Equation (10) then reduces to

$$\omega^2 = \omega_o^2 \left[1 - \frac{\varepsilon_o \varepsilon_r E^2 V}{U_o} \right] \quad (11)$$

where V is the volume of the perturbation in cubic meters. U_o is the energy stored in the empty resonator in Joules. E is the electric field in Volt/meter, and $\varepsilon_o = 8.85 \times 10^{-12}$ Joules/(Volt² · meter). Similar analysis of a loaded cavity resonator has been used to measure the complex electric and magnetic susceptibility of solid samples [22].

3.3. Measurement Method

The energy stored in the resonator, U_o , is related to the unloaded Q of the resonator directly through the definition of unloaded Q

$$Q = \frac{\omega U_o}{P_d} \quad (12)$$

P_d is the microwave power, in Watts, dissipated inside the resonator, which in this case is composed of resistive loss in the copper surfaces. The dissipated power is proportional to, but not equal to, the available power, P_{av} , incident on the resonator

$$P_d = P_{av} \cdot \frac{4 \frac{Q_L}{Q} \left(1 - \frac{Q_L}{Q} \right)}{1 + \frac{\beta_2}{\beta_1}} \quad (13)$$

where Q_L is the measured, or loaded, Q of the resonator, β_1 is the input coupling coefficient, and β_2 is the output coupling coefficient. Loaded Q , $Q_L = f_o/\delta f$, is the ratio of the 3-dB bandwidth of the resonator, δf , to the resonant frequency, and is illustrated in Figure 3(a).

The coupling coefficients, β_1 and β_2 , have values between zero and unity. The coupling coefficient is zero when microwave power is unable to pass from the cable into the resonator. This is the case if the antenna probe either is inadequate in size or is located where there is no field. If the probe is electric in nature, but the resonant mode of the cavity has no electric field at the probe location, then there will be no coupling. The coupling coefficient is unity when power passes completely into the resonator and there is no re-emission or reflection at the coupling port. β_1 and β_2 are determined from the measured reflection coefficients of the resonator. To measure a coupling coefficient, the reflected power is measured with a network analyzer.

When using a scalar network analyzer, a directional coupler is used as shown in Figure 4 to measure the power reflected from the input port of the resonator. The reflected power, plotted in S -parameter form, is depicted on the network analyzer screen in Figure 4 and exhibits a dip at resonance. The depth of the dip, ΔS_{11} or ΔS_{22} , measured in decibels is used to compute the reflection coefficients, $|S_{11}| = 10^{\Delta S_{11}/20}$ and $|S_{22}| = 10^{\Delta S_{22}/20}$, where ΔS_{11} or ΔS_{22} are negative numbers in

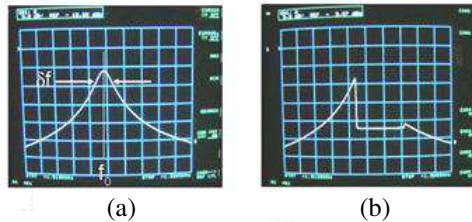


Figure 3. Screen shots of the transmission response viewed with the scalar network analyzer. (a) When the peak electric field at resonance is below E_{BD} the resonator Q and resonance frequency can be measured. (b) When breakdown occurs the transmission response distorts significantly.

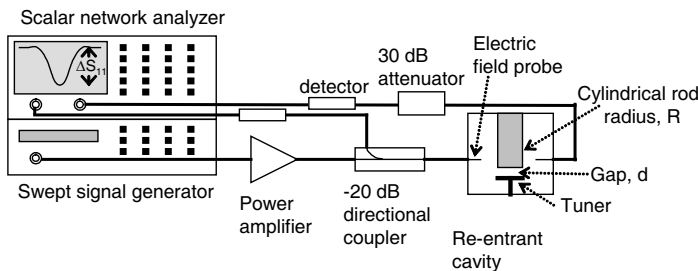


Figure 4. The set-up used to measure the power reflected from, and transmitted through, the re-entrant cavity. The swept signal begins with a hp8350B sweep oscillator. It is amplified by an Amplifier Research 5S1G4 power amplifier. The amplified signal passes backward through a -20 dB directional coupler and reaches the cavity. The microwave amplitude is converted to DC by a hp85025B detector before being displayed on the hp8757C scalar network analyzer. In this depiction, the reflected signal is being displayed as a function of frequency on the scalar network analyzer screen.

decibels. The coupling coefficients are then

$$\beta_1 = \frac{1 - |S_{11}|}{|S_{11}| + |S_{22}|} \quad \beta_2 = \frac{1 - |S_{22}|}{|S_{11}| + |S_{22}|} \quad (14)$$

The coupling coefficients are also useful to compute the unloaded Q used in Equations (12) and (13)

$$Q = Q_L(1 + \beta_1 + \beta_2) \quad (15)$$

To determine the electric field at the location of the perturbation using measured values of f , f_o , β_1 and β_2 , Equation (11) is solved for U_o and substituted into Equation (12). Equation (13) is also substituted into Equation (12), which is then solved for E in Volts/meter

$$E = \sqrt{P_{av} \cdot (f_o - f) \cdot \left[\frac{Q}{\pi f_o^2} \frac{1}{\epsilon_r \epsilon_o V} \frac{4 \frac{Q_L}{Q} \left(1 - \frac{Q_L}{Q}\right)}{1 + \frac{\beta_2}{\beta_1}} \right]} = \sqrt{P_{av} \cdot (f_o - f) \cdot A} \quad (16)$$

where, for lack of any other name, the factor A will be called the “dissipation coefficient”. Q , Q_L , β_1 and β_2 are measured on the unperturbed cavity. It should be remembered that this is for electric perturbations in negligible magnetic field only.

To determine the local electric field at a point inside a cavity resonator, a dielectric of known permittivity, such as PTFE with $\epsilon_r = 2.1$, is placed at the point of interest. The only measurement needed with the dielectric in place is resonant frequency, f , in Hz. With the dielectric then removed, the resonant frequency, f_o , is measured along with Q , Q_L , β_1 and β_2 . Equation (16) is used to calculate the quantity $\sqrt{A \cdot (f_o - f)}$. The electric field is then known for all levels of the available power through $E = \sqrt{P_{av}} \sqrt{A \cdot (f_o - f)}$, where P_{av} is in Watts.

The assumed electric field uniformity cannot be under-emphasized. A simple experimental test for its validity is to repeat the determination of A with a smaller dielectric perturbation. A different resulting value of A , larger or smaller, with a different perturbation size is an indication that E is not uniform.

4. BREAKDOWN MEASUREMENTS AND COMPARISON TO OTHER METHODS

The electric field at breakdown versus pressure is shown in Figure 1 for dry nitrogen. It is important to take steps to ensure that the gas is

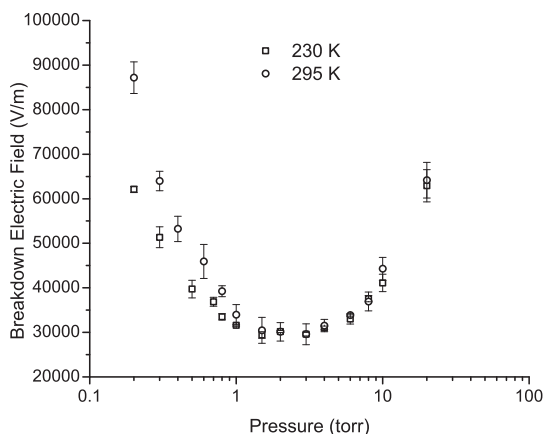


Figure 5. The threshold electric field of nitrogen at 2.76 GHz is affected by water vapor at pressures below the Paschen minimum. At 0.2 torr, the breakdown electric field for cryopumped nitrogen is about 70% that of the breakdown field without cryopumping.

dry. A pressurized cylinder of 99.99% nitrogen is used as a gas source, but water outgases from the chamber walls. Cryopumping is used to eliminate this water as well as hydrocarbons from the vacuum system. The resonant cavity is attached to the cold finger of a cryocooler and its temperature is maintained below 270 Kelvin. For small gaps, the resonance is maintained even with one wall of the resonator housing removed, permitting viewing of the discharge through a window on the vacuum chamber. Breakdown in nitrogen at 2.76 GHz is shown in Figure 5 at room temperature and at 230 K. Temperature dependence is more evident at pressures below the minimum, where the plasma is collisionless, and it is practically absent above the minimum. Varying the temperature in the range of 250 K to 300 K has only been found to influence the results through the condensation of water in the region at and above 273 K, as can be seen for Oxygen breakdown shown in Figure 6.

Pressure was measured using a Pirani gauge attached to a port on the vacuum chamber. A Pirani gauge is factory calibrated for nitrogen and oxygen. However, for other gases, such as helium and carbon dioxide, it has been necessary to apply a manufacturer specified correction to the pressure reading.

The breakdown electric field was measured in the re-entrant resonator at 1.85 GHz. The measurement was repeated at each pressure four to six times, and the uncertainties reflect the error in the

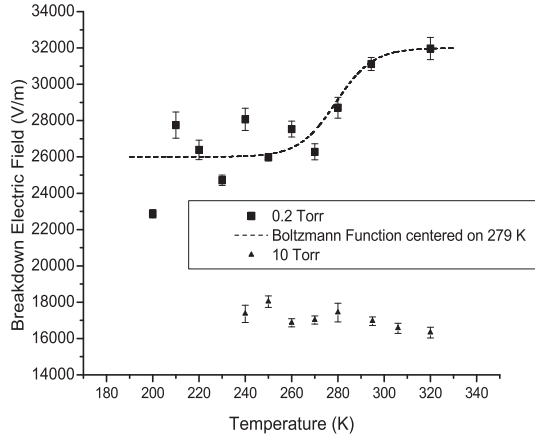


Figure 6. Variation of the breakdown electric field of O_2 with chamber temperature. The dashed line is a sigmoidal overlay illustrating the step in the low pressure curve which starts in the neighborhood of the freezing point of water.

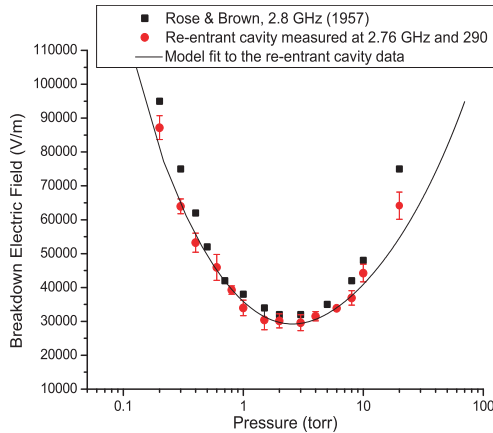


Figure 7. Electric breakdown field (E_{bd}) of molecular nitrogen gas measured in the re-entrant resonator with electric fields calculated from perturbation theory and a fit to Equation (8) with $\chi_R^2 = 1.20$. This is compared to data from Rose & Brown (1957) measured in a parallel plate resonator with electric fields determined analytically. The discrepancies at pressures below 1 torr are likely due to water vapor content of the gas. For both curves, $\Lambda \approx 0.2$ cm.

mean. The gas was purged from the system between each breakdown measurement in order to minimize the background ionization. The 1.85 GHz data in Figure 1 were first fit to Equation (8) using Origin release 8 (OriginLab Corp., Northampton, MA, USA). The fit parameters for this particular curve are $m = 0.48 \pm 03$, $B \approx 10.1 \pm 1.1$ GHz/torr, and $C = 12,478 \pm 759$ V/m·torr^{0.5}. Essentially, we find that the exponent, m , is nominally 1/2. Gurevich's model for air breakdown in open space under traveling waves resembles Equation (8), except that $m = 1$. When $m = 1$, a minimum in breakdown does not occur. The breakdown minimum in the neighborhood of 1 torr is a characteristic of a plasma in a closed capacitive space.

The length of the resonant rod was changed to 20.5 mm, producing a resonance at 2.8 GHz. The breakdown of nitrogen at 2.8 GHz is shown in Figure 7 along with E_{bd} measured by Rose & Brown [23] using a parallel plate copper resonator. The breakdown value depends weakly on the characteristic diffusion length for values of Λ below a few millimeters [10]. For our data, $\Lambda = 0.18$ cm and for Rose and Brown's data, $\Lambda = 0.202$ cm. Rose and Brown's breakdown occurred during the excitation of the TM₀₁₀ mode of a parallel plate resonator, allowing the peak electric field to be calculated analytically, but also resulting in a non-uniform field. The data in Figure 7 were taken at room temperature in order to match the conditions used by Rose and Brown.

Fitting the microwave data for Nitrogen to Equation (8) at 250 Kelvin for values of Λ in the range of 0.09 cm to 0.2 cm, produces the weighted parameter values for nitrogen gas: $m = 0.478 \pm 0.012$ and $B = 8.2 \pm 0.6$ GHz/torr, with no discernable dependence on Λ or frequency. Because of the higher room temperature breakdown value at pressures below the minimum (see Figure 5), the fit parameters are somewhat different at room temperature, especially B which determines the width of the minimum. Using the room temperature fit parameters determined at 1.85 GHz of $m = 0.455$ and $B = 8.0$ GHz/torr in Equation (9) provides the prediction $P_{\min} = (0.879)f$, where f is in GHz and P_{\min} is in torr. Figure 8 shows P_{\min} for N₂ in a room temperature chamber reported by several authors [10, 19] including the values from Figures 1 and 7 of this paper. Each point comes from a different data set, and corresponds to a different value of the characteristic diffusion length, Λ , which varies from 0.2 cm to 2.65 cm. Uncertainties shown for the literature values were based on the precision with which the minimum could be read from a printed graph. The increase in the breakdown pressure minimum with increasing frequency continues on to much higher frequency ranges, though not in a linear manner. Breakdown of nitrogen

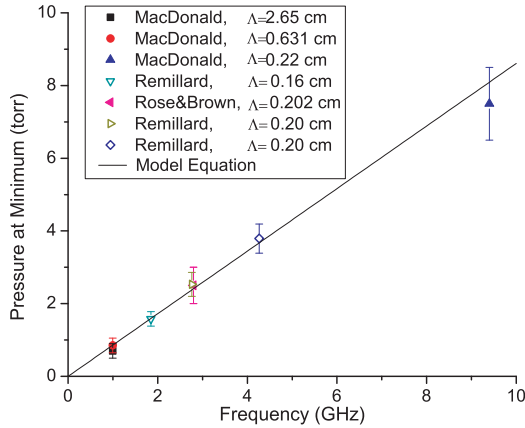


Figure 8. After fitting the N_2 breakdown data at 1.85 GHz, the fit parameters $m = 0.455$ and $B = 8.0 \text{ GHz/torr}$ were used in model Equation (9) to predict the pressure where the breakdown curve is at a minimum. P_{\min} values were taken from the literature and from this work and overlaid on the model equation.

induced at optical frequencies, for example, has a minimum around 76,000 torr [17].

The breakdown pressure minimum of nitrogen is not completely universal. When Λ is less than about 1 mm, the value of P_{\min} appears to drop slightly [24]. The data in Figure 8 show a universality in the transition from a collisionless to a collisional plasma for characteristic diffusion lengths of at least 1.6 mm and larger.

5. CONCLUSION

A method to measure the microwave electric field at breakdown in a re-entrant resonator has been described. Measured threshold fields have been compared to those reported from TM_{010} parallel plate resonators and found to be very similar. A model based on the inefficient response of free electrons to an oscillating electric field was fit to the breakdown curves, suggesting that an appropriate model for microwave breakdown in enclosed spaces (e.g., capacitive discharges) is contained in the equations

$$E_{bd} = CP^{1/2} \sqrt{1 + \frac{\omega^2}{(B \cdot P)^2}} \quad \text{and} \quad P_{\min} = \frac{\omega}{B} \quad (17)$$

where the coefficient, C , may be weakly frequency dependent. Use of the fit parameter, B , to successfully predict the frequency dependence of the pressure where E_{bd} is a minimum provides a self-consistent confirmation of the validity of this model.

Finally, the measurement method and model developed here will be used in a variety of investigations in the pressure regime of the transition between collisional and collisionless microwave breakdown. The emission spectra have been seen to correspond to this transition. For example, the 502 nm emission line of helium gains prominence as the pressure is reduced through the transition, leading to a color change in the plasma. Significant nonlinear distortion of the microwave signal has been found to occur at breakdown, and the degree of even and odd distortion around the minimum will be examined in the near future. Finally, there is significant interest in the breakdown products, in particular ozone generation, which can be examined in the system built in this work.

ACKNOWLEDGMENT

This work was supported by a seed grant from the Michigan Space Grant Consortium, by the National Science Foundation REU grant number 0452206, and by the Hope College Division of Natural and Applied Sciences. The authors thank David Daugherty for fabrication of the resonators.

REFERENCES

1. Matthaei, G., L. Young, and E. M. T. Jones, *Microwave Filters, Impedance-Matching Networks, and Coupling Structures*, Chapter 15, Artech House, Dedham, MA, 1980.
2. Anderson, D., U. Jordan, M. Lisak, T. Olsson, and M. Ålander, "Microwave breakdown in resonators and filters," *IEEE Trans. Microwave Theory and Techniques*, Vol. 47, No. 12, 2547–2556, December 1999.
3. Porteanu, H.-E., S. Kühn, and R. Gesche, "Low-power microwave plasma conductivity," *IEEE Trans. Plasma Sci.*, Vol. 37, No. 1, 44–49, January 2009.
4. Kuo, S. P., "Basis of ionospheric modification by high-frequency waves," *Progress In Electromagnetics Research*, PIER 73, 277–296, 2007.
5. Gurevich, A. V., N. D. Borisov, S. M. Geisse, and P. Hartogs, "Artificial ozone layer," *Phys. Lett.*, Vol. A207, 281–288, 1995.

6. McColl, W., C. Brooks, and M. L. Brake, "Electron density and collision frequency of microwave-resonant-cavity-produced discharges," *J. Appl. Phys.*, Vol. 74, No. 6, 3724–3735, September 15, 1993.
7. Atkins, P., *Physical Chemistry*, 5th Edition, W. H. Freeman & Co., New York, 1994.
8. Sato, M., "Interpretation of argon breakdown in dc and microwave fields," *Bull. Yamagata Univ. (Eng.)*, Vol. 25, No. 2, 119–125, 1999.
9. Margenau, H., "Conduction and dispersion of ionized gases at high frequencies," *Phys. Rev.*, Vol. 69, No. 9–10, 508–513, 1946.
10. MacDonald, A. D., *Microwave Breakdown in Gases*, Wiley, New York, 1966.
11. Radmilović-Radjenović, M., J. K. Lee, F. Iza, and G. Y. Park, "Particle-in-cell simulation of gas breakdown in microgaps," *J. Phys. D: Appl. Phys.*, Vol. 38, 950–954, 2005.
12. Paschen, F., "Über die zum Funkenübergang in Luft, Wasserstoff und Kohlensäure bei verschiedenen Drucken erforderliche Potentialdifferenz," *Annalen der Physik*, Vol. 273, No. 5, 69–96, 1889 (reprinted in the March 16, 2006 German edition).
13. Miller, H. C., "Paschen curve in nitrogen," *J. Appl. Phys.*, Vol. 34, 3418, 1963.
14. Gurevich, A. V., N. D. Borisov, and G. M. Milikh, *Physics of Microwave Discharges: Artificially Ionized Regions in the Atmosphere*, Grodon and Breach, Amsterdam, 1997.
15. Gurevich, A. V., A. G. Litvak, A. L. Vikharev, O. A. Ivanov, N. D. Borisov, and K. F. Sergeichev, "Artificially ionized region as a source of ozone in the stratosphere," *Physics-Uspekhi*, Vol. 43, No. 11, 1103–1123, 2000.
16. Fridman, A. and L. A. Kennedy, *Plasma Physics and Engineering*, Taylor and Francis Books, New York, 2004.
17. Raizer, Y. P., *Gas Discharge Physics*, 143, Springer-Verlag, Berlin, 1991.
18. Kelly, M. B. and A. J. Sangster, "Cylindrical re-entrant cavity resonator design using finite-element simulation," *Microwave and Optical Technol. Lett.*, Vol. 18, No. 2, 112–117, June 5, 1998.
19. Rose, D. J. and S. C. Brown, "Methods of measuring the properties of ionized gases at high frequencies. 2. measurement of electric fields," *J. Appl. Phys.*, Vol. 23, No. 7, 719–722, 1952.
20. Remillard, S. K., P. O. Radzikowski, S. Cordone, D. S. Applegate, A. Mehrotra, J. D. Kokales, and A. Abdelmonem, "A closed slot-

- line resonator filter," *IEEE Microwave and Wireless Components Letters*, Vol. 14, No. 5, 234–236, 2004.
21. Jr. Maier, L. C. and J. C. Slater, "Field strength measurements in resonant cavities," *J. Appl. Phys.*, Vol. 23, No. 1, 68–77, 1952.
 22. Hutcheon, R., M. de Jong, and F. Adams, "A system for rapid measurements of RF and microwave properties up to 1400°C, Part 1: Theoretical development of the cavity frequency-shift data analysis equations," *J. Microwave Power and Electromag. Energy*, Vol. 27, No. 2, 87–92, 1992.
 23. Rose, D. J. and S. C. Brown, "Microwave gas discharge breakdown in air, nitrogen, and Oxygen," *J. Appl. Phys.*, Vol. 28, No. 5, 561–563, 1957.
 24. Herlin, M. A. and S. C. Brown, "Breakdown of a gas at microwave frequencies," *Phys. Rev.*, Vol. 74, No. 3, 291–296, 1948.